

Chaotic Dynamics and Two-Field Inflation

Richard Easther ¹

Department of Physics, Brown University,
Providence, RI 02912, United States of America.

Kei-ichi Maeda ²

Department of Physics, Waseda University,
3-4-1 Okubo, Shinjuku-ku, Tokyo, Japan.

Abstract

We demonstrate the existence of chaos in realistic models of two-field inflation. The chaotic motion takes place after the end of inflation, when the fields are free to oscillate and their motion is only lightly damped by the expansion of the universe. We then investigate whether the presence of chaos affects the predictions of two-field models, and show that chaos enhances the production of topological defects and renders the growth rate of the universe sensitively dependent upon the “initial” conditions at the beginning of the oscillatory era.

¹easther@het.brown.edu

²maeda@mn.waseda.ac.jp

1 Introduction

Inflationary cosmology and chaos theory are sites of intense activity within astrophysics and mathematics. As the equations governing the evolution of an inflationary universe are nonlinear, it is natural to ask whether the insight gained from studies of chaos in systems of differential equations sheds any light upon the behavior of the inflationary universe. In this paper we present *prima facie* evidence that the dynamics of realistic inflationary cosmological models based on two coupled scalar fields can be chaotic.¹

Chaotic dynamics in models consisting of a single (non-minimally coupled) scalar field in a Robertson-Walker background have been studied by several authors [2, 3, 4, 5]. Moreover, Cornish and Shellard [6] show that the familiar inflationary model of a minimally coupled field with a quadratic potential exhibits chaotic dynamics when spacetime has positive spatial curvature.

In chaotic models with just one scalar field the scale factor must always be an intrinsic part of the chaotic system; thus, the timescale over which chaos becomes manifest is roughly defined by the lifetime of the universe. Cornish and Levin [7] point out that in two-field models the oscillations of the fields can be the primary source of chaos, so chaotic effects can become significant on comparatively short timescales. However, their analysis hinges on the dependence of the final state of the universe on the initial conditions, so their work does not fully realize the possibility that the timescale associated with chaos in two-field inflation can be much less than the lifetime of the universe. Hence, while chaos has been found in several homogeneous inflationary models, it would typically only be detectable by an “observer” able to study either a large ensemble of universes, or the same universe during more than one cycle of expansion and contraction. A different situation arises in analyses of reheating, when the inflaton decays into a second scalar field [8, 9, 10]. At least one of the fields is expanded in terms of its spatially dependent modes, so the resulting dynamical system is more complex than in the homogeneous case. However, small changes in the model parameters can cause massive variations in the occupation numbers associated with the modes, which is the qualitative behavior associated with chaos.

The chaotic motion we examine is derived from the homogeneous equations of motion and takes place in a well-defined era after the end of inflation. Consequently, the chaotic period we identify can, in principle, have effects which are observable from within the present-day universe. Furthermore, previously studied examples of chaos in

¹Inflationary models with chaotic dynamics, which are sensitively dependent upon their initial conditions, are not necessarily synonymous with chaotic inflationary models [1], which are recommended, in part, by their relative insensitivity to initial conditions.

homogeneous inflationary models typically depend upon non-zero spatial curvature, a cosmological constant, or a non-minimal coupling between the fields and the gravitational sector. All these terms are absent from our model, and the inflationary system we analyze has already received considerable attention because of its promising cosmological predictions. The only additional assumption we need is that the parameter values and couplings between the scalar fields and the rest of the matter sector (which we do not include explicitly) permit a sufficiently long and lightly damped oscillatory period for the chaotic effects to become manifest.

We begin by analyzing the evolution of the fields in the limiting case when the friction term arising from the expansion of the universe is absent from the equations of motion for the fields. We demonstrate that this system is chaotic, and that there is a minimum energy below which chaos does not occur. When the friction term is restored, we show that the energy changes slowly on a time scale defined by the typical oscillation period in the post-inflationary era. The chaotic properties of the system persist, but are now transient and cease to be apparent once the energy drops below the critical value needed for chaos.

If inflation is the source of the fluctuations that seed structure formation, the “initial conditions” of the many post-inflationary horizon volumes accessible to a present-day observer cannot have been strictly identical. However, analyses of inflationary models usually make the tacit assumption that small differences in field values and velocities between post-inflation horizon volumes can be ignored when computing “zero order” quantities such as the scale factor. The validity of this assumption cannot be taken for granted in the presence of chaos. In particular, we consider whether chaotic motion enhances the production of topological defects, and if there is a well-defined relationship between the expansion of the universe and the decrease in density during the chaotic era.

2 The Model and the Equations of Motion

The equations of motion for inflationary models minimally coupled to Einstein gravity are well known, and for two scalar fields with a combined potential $V(\phi, \psi)$ they take the form

$$H^2 = \left(\frac{\dot{a}}{a}\right)^2 = \frac{8\pi}{3m_{\text{pl}}^2} \left[\frac{\dot{\phi}^2}{2} + \frac{\dot{\psi}^2}{2} + V(\phi, \psi) \right], \quad (1)$$

$$\frac{\ddot{a}}{a} = \frac{8\pi}{3m_{\text{pl}}^2} \left[V(\phi, \psi) - \dot{\phi}^2 - \dot{\psi}^2 \right], \quad (2)$$

$$\ddot{\phi} = -3H\dot{\phi} - \frac{\partial V}{\partial \phi}, \quad (3)$$

$$\ddot{\psi} = -3H\dot{\psi} - \frac{\partial V}{\partial \psi}, \quad (4)$$

where a is the scale factor of the Robertson-Walker spacetime metric, m_{pl} is the Planck mass, and dots denote differentiation with respect to time. The specific model we consider is defined by the potential

$$V(\phi, \psi) = \left(M^2 - \frac{\sqrt{\lambda}}{2} \psi^2 \right)^2 + \frac{m^2}{2} \phi^2 + \frac{\gamma}{2} \phi^2 \psi^2, \quad (5)$$

where we assume that $\gamma \geq 0$. The inflationary properties of this potential have been widely studied [11]-[21]. Inflation is driven by the ϕ field: when ϕ is large, ψ acquires a large positive effective mass, and the fields roll down the $\psi \approx 0$ groove in the potential. There are two distinct inflationary modes, which Copeland *et al.* [17] dub the *inflaton dominated* and *vacuum dominated* regimes. In the former case, the total energy density is much greater than M^4 , while during vacuum dominated expansion the energy density is of the order of M^4 . The degenerate minima located at $\phi = 0$ and $\psi = \pm M\sqrt{2\lambda}^{-1/4}$ (separated by a barrier of height M^4) can lead to the formation of topological defects.

The inflationary dynamics associated with this potential are described in [17], and we summarize them here. The effective mass of the ψ field becomes zero when $\phi^2 = \phi_{\text{inst}}^2$, where

$$\phi_{\text{inst}}^2 = \frac{2\sqrt{\lambda}M^2}{\gamma}. \quad (6)$$

When ϕ^2 first drops below ϕ_{inst}^2 , ψ is balanced on an unstable local maximum in the potential and becomes free to oscillate. Conversely, during inflation $\psi \approx 0$ and the potential reduces to the single field case,

$$V(\phi) \approx M^4 + \frac{m^2}{2} \phi^2. \quad (7)$$

If inflation ends with $\phi^2 \gg \phi_{\text{inst}}^2$, the M^4 term can be ignored during inflation, which ceases when

$$\phi_{\text{end}}^2 \approx \frac{m_{\text{pl}}^2}{4\pi}, \quad (8)$$

and the slow roll conditions are no longer satisfied. If inflation continues until $\phi^2 \sim \phi_{\text{inst}}^2$, it ends quickly via the instability in the ψ field. A realistic model in which inflation ends with the universe in the inflaton dominated stage must satisfy

$$4\sqrt{\pi} \frac{M}{m_{\text{pl}}} \ll 3 \times 10^{-3}, \quad (9)$$

$$\frac{\gamma}{\sqrt{\lambda}} > 8\pi \frac{M^2}{m_{\text{pl}}^2}, \quad (10)$$

$$m = \frac{5.5 \times 10^{-6}}{\sqrt{8\pi}} m_{\text{pl}}. \quad (11)$$

The first inequality ensures that the M^4 contribution can be ignored, the second guarantees that slow rolling is violated and inflation ends when $\phi^2 > \phi_{\text{inst}}^2$, and the last gives COBE-normalized density perturbations.²

3 The Frictionless Case

We are concerned with the epoch in which the fields are weakly damped and free to oscillate. We begin our analysis by investigating the completely frictionless system. Physically, this is equivalent to assuming that the universe is not expanding and that the energy density is static. Mathematically, this means the equations of motion for the fields can be derived from a Hamiltonian. The equations of motion simplify further if we rescale the variables:

$$\phi = \frac{M^2}{m} \Phi, \quad \psi = \frac{M}{\lambda^{1/4}} \Psi, \quad t = M^2 T, \quad \gamma = \Gamma \frac{\sqrt{\lambda} m^2}{M^2}. \quad (12)$$

The potential becomes

$$V(\Phi, \Psi) = M^4 \left[\left(1 - \frac{\Psi^2}{2}\right)^2 + \frac{\Phi^2}{2} + \frac{\Gamma}{2} \Phi^2 \Psi^2 \right] \quad (13)$$

and the equations of motion are

$$\frac{d^2 \Phi}{dT^2} = -\frac{1}{M^4} \frac{\partial V}{\partial \Phi}, \quad (14)$$

$$\frac{d^2 \Psi}{dT^2} = -\frac{1}{M^4} \frac{\partial V}{\partial \Psi}, \quad (15)$$

$$\frac{E}{M^4} = \frac{1}{2} \left(\frac{d\Phi}{dT}\right)^2 + \frac{1}{2} \left(\frac{d\Psi}{dT}\right)^2 + \frac{V}{M^4}, \quad (16)$$

where E is conserved. These equations are independent of M , so we fix $M = 1$ for convenience. If $\Gamma = 0$, we have a special case: the equations separate and our two dimensional system has two constants of the motion, ensuring that it is integrable [22], and therefore not chaotic. To our knowledge, Hamiltonian chaos associated with the potential described by equation (13) has not been considered before. However, Matinyan

²The numerical value is taken from [17], and would be modified slightly by using the four year COBE result. However, the difference will not affect our work.

and Müller [23] discuss a system which lacks the $\Phi^2/2$ term in the potential but is otherwise equivalent to our model in the absence of friction. In general, Hamiltonian systems with terms like $\Phi^2\Psi^2$ are non-integrable, and Steeb *et al.* summarize discussions of chaotic behavior when the potential consists solely of a $\Phi^2\Psi^2$ term [24].

3.1 Applying the Toda-Brumer Test

The Toda-Brumer test [25, 26] checks for the presence of a growing, unstable solution, which is typically a prerequisite for chaos.³ The criterion for instability is the existence of Φ and Ψ for which

$$\|V''_{\Phi\Psi}\| = \frac{d^2V}{d\Phi^2} \frac{d^2V}{d\Psi^2} - \left(\frac{d^2V}{d\Phi d\Psi} \right)^2 < 0. \quad (17)$$

Inserting equation (13) into equation (17) gives

$$\|V''_{\Phi\Psi}\| = (\Gamma\Psi^2 + 1)(3\Psi^2 - 2) + \Gamma\Phi^2(1 - 3\Gamma\Psi^2). \quad (18)$$

Setting equation (18) to zero and solving gives a parametric equation for the borders of the region within which $\|V''_{\Phi\Psi}\|$ is negative,

$$\Phi^2 = \frac{(3\Psi^2 - 2)(\Gamma\Psi^2 + 1)}{\Gamma(3\Gamma\Psi^2 - 1)}. \quad (19)$$

Inserting this value of Φ into $V(\Phi, \Psi)$ yields $U(\Psi)$, the value of the potential on the boundary of the instability region,

$$U(\Psi) = \left(1 - \frac{\Psi^2}{2} \right) + \frac{1}{2\Gamma} \frac{(3\Psi^2 - 2)(1 + \Gamma\Psi^2)^2}{3\Gamma\Psi^2 - 1}. \quad (20)$$

Minimizing $U(\Psi)$ subject to the constraint that Φ is positive returns the minimum energy (as a function of Γ) needed for instability. When $\Psi^2 = 2/3$, $\Phi = 0$ and $U = 4/9$, putting an upper bound on the minimum energy, which must be non-zero because $\|V''_{\Phi\Psi}\|$ is positive at the minima of the potential. More precisely, solving $U'(\Psi) = 0$ shows that $U(\Psi)$ has extremal values at

$$\Psi^2 = \frac{4}{9} + \frac{1}{9\Gamma} \pm \frac{\sqrt{(2\Gamma - 1)(2\Gamma - 7)}}{9\Gamma}, \quad (21)$$

where we have ignored two roots for which Ψ is imaginary. A little analysis shows that when $\Gamma \leq 9/2$, the minimum energy for instability is $4/9$, corresponding to $\Phi^2 = 0$. For

³The Toda-Brumer criterion is equivalent to the Gaussian curvature of the potential being negative. However, even if $\|V''_{\Phi\Psi}\|$ is never negative chaos can still occur, so the Toda-Brumer test does not provide a sufficient condition for stability.

$\Gamma > 9/2$ the minimum energy for instability is found when Ψ^2 is given by equation (21), with the positive sign on the square root. As $\Gamma \rightarrow \infty$, the minimal value approaches $11/27$, reproducing the result of Matinyan and Müller in the absence of the $\Phi^2/2$ term.

3.2 Lyapunov Exponents

The Toda-Brumer test predicts instability above a critical energy, and other studies show that the coupling between the two fields usually leads to chaos. However, we wish to confirm this explicitly for the potential we consider, and to ascertain the parameter values which are likely to produce cosmologically significant chaos.

We do this by considering the Lyapunov exponents [27]. These are directly related to the fundamental definition of a chaotic system: sensitive dependence upon initial conditions. A system with an n dimensional phase space has n Lyapunov exponents. These measure the logarithm of the expansion of a small n -volume of phase space when it is propagated forwards in time by the equations of motion. In a chaotic system, this region will be stretched exponentially in at least one direction, and the signature of this is a positive maximal Lyapunov exponent. In Hamiltonian systems, the total phase space volume is conserved, leading to a spectrum of Lyapunov exponents that has the form $\lambda_1, \lambda_2, \dots, -\lambda_2, -\lambda_1$, [22]. A corollary is that if a Hamiltonian system is not chaotic all of its Lyapunov exponents are zero. Since the Lyapunov exponents come in pairs with the same magnitude and opposite signs we can check that the values of the exponents we compute numerically are self-consistent.

We calculate the Lyapunov exponents using the algorithm developed by Wolf *et al.* [28] which produces the full spectrum of n exponents at the expense of solving $n^2 + n$ differential equations. In our case, $n = 4$, so the cost of calculating all the exponents is not prohibitive. However, Lyapunov exponents are defined by a limit as $t \rightarrow \infty$ but the numerical integrations only run for a finite time. Hence our numerical estimates of the Lyapunov exponents are never precisely zero in non-chaotic cases. In practice, we continue the numerical integrations long enough to ensure that if $\lambda_1 > 0.005$ and λ_1 and $|\lambda_4|$ differ by less than 1% the system is unambiguously chaotic.

The maximal Lyapunov exponent as a function of E and Γ is displayed in fig. (1), while fig. (2) shows the region of parameter space for which chaos is observed. If $\Gamma \lesssim 0.05$, Φ and Ψ are weakly coupled and the system is typically not chaotic. However, when $E \gtrsim 2$ and $\Gamma \gtrsim 0.05$ then we usually (but not always) find chaos. We very rarely found chaos with $E \lesssim 1$ and never observed chaos with an energy below the minimum value for instability obtained from the Toda-Brumer test. Furthermore, the boundary of the region in parameter space which gave rise to chaos is not smooth, so a small

change in parameter values could bring about a large change in the qualitative nature of the dynamics. For fixed E and Γ only a subset of all the possible orbits in phase space will exhibit sensitive dependence, so the precise forms of figs (1) and (2) depend on the chosen initial data.

4 Chaotic Motion and Inflation

Having demonstrated the existence of chaos in the Hamiltonian system derived from the two-field potential, equation (13), we now turn to the corresponding inflationary model based on the potential, equation (5). Because of the terms proportional to H in equations (3) and (4), the energy density is strictly decreasing. If the energy changes slowly compared to the typical oscillation time of the fields, the friction term is a small perturbation to the Hamiltonian system. Since there is a lower bound on the energy at which the potential, equation (13), can exhibit chaotic motion, any chaos seen in the inflationary dynamics is transient, switching off once the energy drops below the critical value.

In general, the oscillatory phase begins with $\psi \sim 0$ and $\phi^2 \sim \phi_{\text{inst}}^2$, although inflation may cease long before this condition is fulfilled. We define E_{inst} , the (potential) energy at the beginning of the oscillatory epoch,

$$E_{\text{inst}} = V(\phi_{\text{inst}}, 0) = M^4 \left(1 + \frac{\sqrt{\lambda} m^2}{\gamma M^2} \right) = M^4 \left(1 + \frac{1}{\Gamma} \right). \quad (22)$$

where Γ is given by equation (12). The rate of change in the energy density is

$$\frac{dE}{dt} = \frac{d}{dt} \left(\frac{\dot{\phi}^2}{2} + \frac{\dot{\psi}^2}{2} + V(\phi, \psi) \right) = -3H(\dot{\phi}^2 + \dot{\psi}^2), \quad (23)$$

where the second equality uses the equations of motion. During the oscillatory phase $(\dot{\phi}^2 + \dot{\psi}^2) \sim E$. If we assume that $M \sim m$, the characteristic oscillation period of the fields when $E < E_{\text{inst}}$ and $E \sim M^4$ will be on the order of $1/M$. Thus ΔE , the energy lost during a typical oscillation, is roughly

$$\frac{\Delta E}{E} \sim \sqrt{24\pi} \frac{M}{m_{\text{pl}}}. \quad (24)$$

Even if E_{inst} is only a few times larger than M^4 , and $M \sim m \approx 10^{-6} m_{\text{pl}}$, the fields will make tens of thousands of oscillations as the energy decreases from E_{inst} to M^4 , when symmetry breaking occurs. This estimate is confirmed by direct numerical computation. Thus the friction term is much smaller than the other terms in the equations of

motion, and the energy loss per cycle can easily be as low as 1 part in 10^5 . It is likely that the chaos seen in the Hamiltonian dynamics will survive the addition of such a small perturbation.

We now turn our attention to the phenomenological aspects of chaos in the post-inflationary universe. We consider two ways in which the chaotic motion we have observed in the Hamiltonian dynamics could influence the observable properties of the universe: by enhancing the production of topological defects in the early universe, or by introducing stochastic variations into the relationship between length scales at the present epoch and the horizon size during inflation.

The smallness of the perturbation caused by the friction term creates a practical difficulty. Tracing the evolution of the fields through tens of thousands of oscillations is computationally expensive and, because the underlying system is chaotic, would require an unrealistic level of numerical precision. This problem is accentuated when we consider the evolution for many different choices of initial conditions. Thus we wish to make the friction more efficient while still ensuring that it is sub-dominant, so that the numerical calculations are tractable. We could do this by adding a coupling between the fields and radiation, in a manner analogous to that discussed by Albrecht *et al.* [29]. Alternatively, we can consider oscillatory motion at an energy scale considerably higher than that consistent with COBE so that H , which is proportional to the the square root of the energy density, is larger and the damping more efficient [30]. Both approaches reduce the length of the chaotic era, and therefore reduce the impact of the chaotic dynamics. We adopt the latter technique, as it does not alter the structure of the equations, and work with $M = m = 1$, $\lambda = 1$, $\gamma = .5$ and $m_{\text{pl}} = 5 \times 10^3 m$. We begin our integrations with $E \approx E_{\text{inst}} = 3M^4$. The typical duration of the oscillatory era is a few hundred oscillation times. The growth of the universe during the oscillatory era is not significantly changed by the scaling.

4.1 Defect Formation

Traditionally, only inflationary models which ended with a first order phase transition were thought to produce topological defects at the end of inflation. One of the new features of two-field inflation was that it can easily produce topological defects after a second order transition, provided the potential has more than one distinct vacuum, like the case we consider here.

In fig. (3) we show the relationship between the sign of ψ field at late times and the “initial” conditions that apply when $E \approx E_{\text{inst}}$. We have to chosen to vary the initial velocities, while keeping the other parameters fixed. With $\gamma = 0.5$ we see that even very

small changes in the initial conditions change the minimum of the potential picked out by ψ after symmetry breaking. Conversely, with $\gamma = 0$ large changes in the initial data are required to alter the final state, and there are sharp boundaries between regions of initial conditions space leading to different minima. This qualitative difference is attributable to the fact that with $\gamma = 0.5$ we have transient chaos, whereas in the absence of friction the underlying dynamics are integrable with $\gamma = 0$.

The difference in initial energy between the different configurations with $\gamma = 0.5$ is $\delta E/E \lesssim 10^{-4}$, slightly more than that suggested by COBE, so the range of initial densities is not unreasonably large. The spread in energies for the initial conditions examined with $\gamma = 0$ is much wider, giving $\delta E/E \lesssim 5 \times 10^{-2}$.

We have chosen to work with parameters that lead to a much shorter oscillatory period than would be found with realistic values, so we *underestimate* the impact of the chaotic period. Furthermore, if ϕ had rolled freely from the end of inflation its velocity would be much greater than the range of values we considered. This causes us to underestimate the initial energy and further reduces the duration of the chaotic era. On the other hand, we have ignored couplings between the scalar fields and the rest of the matter sector and spatial gradients in the fields. Incorporating these effects would provide additional friction which damps the oscillations of the ϕ and ψ and therefore tends to suppress their chaotic motion.

Because we do not include gradient terms, the plots in fig. (3) represent the symmetry breaking pattern for an ensemble of homogeneous universes (or horizon volumes), rather than for a single universe in which the field values vary significantly within a single horizon volume. Thus, we do not claim that the results obtained here are directly applicable to the rate of defect formation in the real universe. However, it is clear that two correlated horizon volumes which have not been in causal contact since the end of inflation are much less likely to remain correlated after symmetry breaking if the dynamics of the oscillatory phase permit transient chaos. Thus the chaotic properties of two-field inflation can be expected to enhance the level of defect production.

These numerical results apply to a specific set of parameters, but in general the post-inflationary universe will be chaotic if the energy density at the beginning of the oscillatory period is high enough to produce chaos in the corresponding frictionless system. Thus transient chaos is a possibility if the parameters combine to give $\Gamma \gtrsim 0.05$ and the energy density is greater than approximately $2M^4$ at the end of inflation. If inflation ends with the universe in the inflaton dominated regime, $\dot{\phi}^2$ will be similar in size to E_{inst} , equation (22), at the beginning of the oscillatory era and the energy requirement will almost certainly be satisfied. However, if inflation lasts

into the vacuum dominated regime the energy density at the end of inflation could be close to M^4 , which would not be high enough for chaos even if Γ , the rescaled coupling between the fields, was large.

4.2 The Growth of the Scale Factor

To make predictions from inflationary models we need to match comoving distances in the present universe to the comoving horizon size during inflation. The precise form of this relationship depends on the thermal history and effective equation of state that applies after the end of inflation [31, 32]. Derivations of this relationship typically assume that the many post-inflation horizon volumes contained within the visible universe have grown by the same amount since inflation stopped. This assumption seems reasonable, as microwave background data suggests that the primordial universe is homogeneous to within 1 part in 10^{-5} . However, a period of transient chaos can massively amplify small differences in initial conditions, so we now explicitly examine this assumption by studying the growth of the scale factor during the interval in which the energy density evolves from E_{inst} to M^4 . We use the same sets of initial conditions considered in the previous subsection.

In fig. (4) we plot the magnitude of the scale factor, a , when $E = M^4$, where $a = 1$ when $\phi = \phi_{\text{inst}}$. In the chaotic case, an initial variance in the energy of less than .01% leads to differences of over 10% in the size of the universe at symmetry breaking. In the non-chaotic case the growth of the universe varies much less dramatically as the initial velocities of the fields are altered, and what difference we do see is attributable to the variation in initial energy corresponding to the different initial velocities. Moreover, in the non-chaotic case the growth of the universe between the start of the integration and symmetry breaking is a smooth function of the initial data, while for the chaotic case it is not.

The chaotic case produces large variations in the scale factor because the precise mixture of kinetic and potential energy varies significantly with small changes in the initial conditions, as the fields settle into different meta-stable oscillatory modes. In turn, this alters the effective equation of state and the amount of growth that occurs as the energy density drops from E_{inst} to M^4 . This is illustrated by fig. (5), where the evolution of ψ is plotted for two slightly different sets of initial conditions. Obviously, the solutions diverge after a few oscillations, which is a consequence of the chaotic dynamics. Less dramatically, both solutions settle into a quasi-stable oscillatory mode, but the amplitude of the oscillations differs significantly between the two solutions. It is the latter difference that changes the average kinetic and potential energies. This effect

does not rely on the potential having more than one vacuum, which is a prerequisite for the formation of topological defects, but could occur in any two-field model with transient chaos.

In practice, the variation in the scale factor due to chaotic motion occurring after inflation could introduce a stochastic term into estimates of the growth of the universe since the end of inflation. In turn, this would affect estimates of the power associated with the primordial fluctuations on different length scales, assuming that the fluctuations generated during inflation differ from the perfectly scale-free Harrison-Zel'dovich spectrum. The typical length over which the scale factor varies will be on the order of the horizon size at the end of inflation, which is vastly smaller than astrophysical length scales in the present universe. However, models which allow a short burst of inflation after the main period of inflation is over, such as thermal inflation [33] or more complicated two-field models [34], could conceivably magnify the post-inflationary horizon volumes to the point where the stochastic properties of the scale factor would not be smeared out on astrophysical lengthscales.

5 Discussion

We have shown that the dynamics of the post-inflationary era in two-field inflation can be chaotic. We initially analyzed the evolution of the fields in the frictionless limit corresponding to a static spacetime background. This reduced the equations of motion for the fields to a two-dimensional Hamiltonian system. By employing the Toda-Brumer test and calculating the Lyapunov exponents we demonstrated that the frictionless system is chaotic. This approach is free from many of the difficulties associated with chaos in general relativity, especially the co-ordinate dependence of the Lyapunov exponents, as discussed by Rugh [35]. We then demonstrated that the damping term induced by the expansion of the universe can be viewed as a small perturbation to the post-inflationary dynamics, and that the most important qualitative property of chaos - sensitive dependence on initial conditions - persists when the fields evolve in an expanding universe. The chaotic era is transient and lasts from the beginning of the oscillatory period, which commences when the effective mass squared of the ψ field becomes negative, until the energy density, which is strictly decreasing, drops below the critical value needed to sustain chaos.

Our analysis is based on a specific potential, which we chose because its inflationary properties had already received widespread attention, and because it allowed us to investigate the formation of topological defects after the end of inflation. From the

perspective of the idealized, frictionless dynamics chaos is endemic in two-field models with couplings like $\gamma\phi^2\psi^2$. Thus we expect that the type of chaos described here could arise in any inflationary model with two coupled fields which undergo lightly damped oscillations.

In models of reheating and particle production based on parametric resonance the inflaton field is coupled to another boson, usually a scalar, and the resulting system is similar (and sometimes identical) to the two-field model considered in this paper. Refs [8, 9, 10] show that particle production during reheating can depend delicately upon the model parameters, which is the qualitative behavior associated with chaos. These calculations expand the field(s) in terms of their spatially dependent modes, so the underlying dynamical system is more complex than the homogeneous case discussed here. However, the link between the chaos we have demonstrated in the homogeneous equations of motion and the phenomenology of reheating is extremely intriguing.

In practice there are several ways in which chaos might be suppressed in a realistic model of two-field inflation; for instance, the parameter values could ensure that the oscillatory period does not begin until the energy density is too low to permit chaos, or the couplings between the scalar fields and other parts of the matter sector may ensure that the oscillations are always strongly damped. Conversely, our numerical integrations were performed with an artificially large damping term, and the parameter values we chose ensured that the oscillatory period did not begin until the energy density was close to the height of the barrier between the two vacua in the potential. Restoring a realistic damping term or increasing the energy density at which oscillations begin would make the chaotic period last much longer than it does in the case considered here.

We have not included spatial variations in the fields, or couplings between the scalar fields and other forms of matter. Thus we cannot determine whether a chaotic period necessarily leads to detectable effects, and if these effects are useful to the model builder, or in conflict with observational evidence. However, our work shows that it is feasible for chaotic effects to influence the observable properties of two-field models. Thus, approximations which do not preserve the chaotic properties of the full system could lead to spurious conclusions about the phenomenology of two-field inflation. It will obviously be important to investigate these issues in more detail.

Inflationary models based on a single scalar field in a spatially flat background do not possess enough degrees of freedom to become chaotic. Since spatial curvature is negligible after inflation, a chaotic era at the end of inflation requires two or more scalar fields. Thus any distinctive observable effects associated with the period of transient

chaos we have identified could provide a mechanism for testing a broad class of two-field models, in the same way that constraints on the scalar and tensor perturbation spectra test a large group of models with a single slowly rolling field [36]. Furthermore, chaotic effects are often associated with fractal structures. Due to the complex nonlinear dynamics associated with defect formation, cosmic string networks have a fractal geometry [37, 38], while stochastic inflationary models have a fractal structure at scales much larger than a typical horizon [39]. Thus we speculate that a chaotic era at the end of inflation may give rise to fractal structure, in which case two-field models of inflation could make testable predictions about the fractal properties of the universe at large scales.

We believe that the scenario analyzed here is the most interesting example of chaotic dynamics in an inflationary model to date. We have found chaos in a model that has already been widely studied because of its promising phenomenology, and we did not need to include non-minimal couplings or non-zero spatial curvature to ensure the presence of chaos. Because of the sensitive dependence of chaotic systems, small differences in the initial conditions which apply at the beginning of the oscillatory epoch can have a significant impact on the subsequent evolution, affecting “zero order” quantities such as the scale factor and the minimum of the potential that the fields evolve towards. Moreover, because the chaotic era occurs after the end of inflation its effects might, in principle, be detectable by human observers.

Acknowledgments

This work was partially supported by a Grant-in-Aid for Scientific Research Fund of the Ministry of Education, Science and Culture (Specially Promoted Research No. 08102010), and the Waseda University Grant for Special Research Projects. RE is supported by DOE contract DE-FG0291ER40688 (Task A), and thanks Cornell University for its hospitality while part of this work was carried out. Computational work in support of this research was performed at the Theoretical Physics Computing Facility at Brown University. We thank Robert Brandenberger and David Wands for their comments on a draft of this paper.

References

- [1] A. D. Linde, *Phys. Lett. B* **129**, 177 (1983).
- [2] E. Calzetta and C. El Hasi, *Class. Quantum Grav.* **10**, 1825 (1993).

- [3] E. Calzetta and C. El Hasi, Phys. Rev. D **51**, 2713 (1995).
- [4] L. Bombelli, F. Lombardo, and M. Castagnino, gr-qc/9707051 (1997).
- [5] A. Helmi and H. Vucetich, gr-qc/9705009 (1997).
- [6] N. J. Cornish and E. P. S. Shellard, gr-qc/9708046 (1997).
- [7] N. J. Cornish and J. J. Levin, Phys. Rev. D **53**, 3022 (1996).
- [8] L. Kofman, A. Linde, and A. Starobinsky, Phys. Rev. D **56**, 3258 (1997).
- [9] P. B. Greene, L. Kofman, A. Linde, and A. A. Starobinsky, Phys. Rev. D **56**, 6175 (1997).
- [10] B. R. Greene, T. Prokopec, and T. Roos, Phys. Rev. D **56**, 6484 (1997).
- [11] L. A. Kofman and A. D. Linde, Nucl. Phys. B **282**, 555 (1987).
- [12] L. A. Kofman and D. Y. Pogosyan, Phys. Lett. B **214**, 508 (1988).
- [13] D. S. Salopek, J. R. Bond, and J. M. Bardeen, Phys. Rev. D **40**, 1753 (1989).
- [14] L. Kofman, Phys. Scr. **T36**, 108 (1991).
- [15] A. D. Linde, Phys. Lett. B **259**, 38 (1991).
- [16] A. Linde, Phys. Rev. D **49**, 748 (1994).
- [17] E. J. Copeland, A. R. Liddle, D. H. Lyth, E. D. Stewart and D. Wands, Phys. Rev. D **49**, 6410 (1994).
- [18] J. García-Bellido and D. Wands, Phys. Rev. D **54**, 7181 (1996).
- [19] J. García-Bellido, A. Linde, and D. Wands, Phys. Rev. D **54**, 6040 (1996).
- [20] J. García-Bellido and A. Linde, Phys. Lett. B **398**, 18 (1997).
- [21] J. García-Bellido and A. Linde, Phys. Rev. D **55**, 7480 (1997).
- [22] E. Ott, *Chaos in Dynamical Systems* (Cambridge University Press, Cambridge, 1993).
- [23] S. G. Matinyan and B. Müller, hep-th/9610233 (1996).
- [24] W.-H. Steeb, C. M. Villet, and A. Kunick, J. Phys. A **18**, 3269 (1985).

- [25] M. Toda, Phys. Lett. A **48**, 335 (1974).
- [26] P. Brumer, J. Comp. Phys. **14**, 391 (1974).
- [27] G. L. Baker and J. P. Gollub, *Chaotic dynamics: an introduction*, 2 ed. (Cambridge University Press, Cambridge, UK, 1996).
- [28] A. Wolf, J. B. Swift, H. L. Swinney, and J. A. Vastano, Physica D **16**, 285 (1985).
- [29] A. Albrecht, P. J. Steinhardt, M. S. Turner, and F. Wilczek, Phys. Rev. Lett. **48**, 1437 (1982).
- [30] A. Albrecht, R. Brandenberger, and R. Matzner, Phys. Rev. D **35**, 429 (1987).
- [31] A. R. Liddle and D. H. Lyth, Phys. Rep. **231**, 1 (1993).
- [32] M. S. Turner, Phys. Rev. D **48**, 3502 (1993).
- [33] D. H. Lyth and E. D. Stewart, Phys. Rev. D **53**, 1784 (1996).
- [34] D. Roberts, A. R. Liddle, and D. H. Lyth, Phys. Rev. D **51**, 4122 (1995).
- [35] S. E. Rugh, in *Deterministic Chaos in General Relativity*, edited by D. Hobill, A. Burd, and A. Coley (Plenum Press, New York, 1994), pp. 359–422.
- [36] J. E. Lidsey *et al.*, Rev. Mod. Phys. **69**, 373 (1997).
- [37] T. Vachaspati and A. Vilenkin, Phys. Rev. D **30**, 2036 (1984).
- [38] H. Pagels, Phys. Rev. D **35**, 1141 (1987).
- [39] M. Aryal and A. Vilenkin, Phys. Lett. B **199**, 351 (1987).

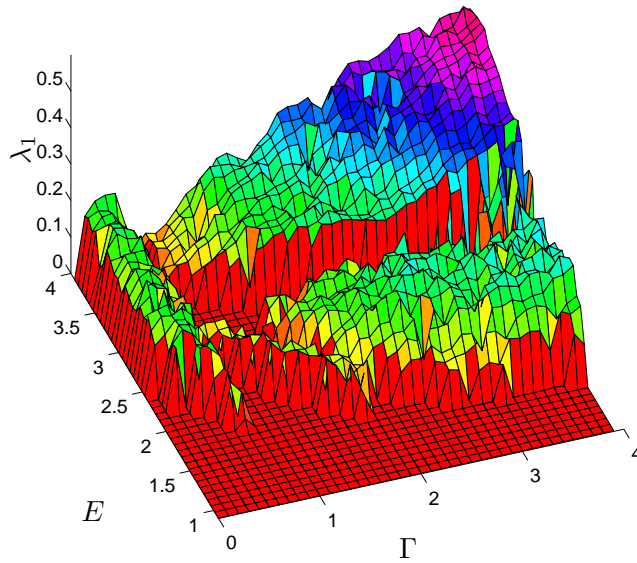


Figure 1: Maximal Lyapunov exponent, λ_1 as a function of energy and Γ . The specific initial data chosen for the integrations was $\Phi = 1$, $\Psi = 1/\sqrt{2}$ and $\dot{\Psi} = 0.64\dot{\Phi}$. The magnitude of the velocities is then fixed by E , and their signs were chosen to be positive.

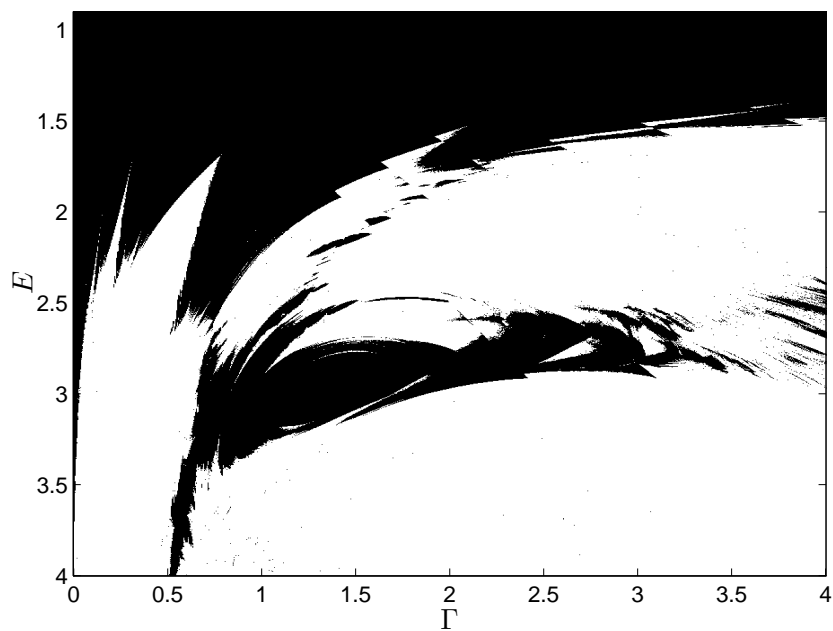


Figure 2: Region of parameter space for which chaos was detected (white points), with the same parameters as used in fig. (1), for a grid of 840×840 equally spaced points.

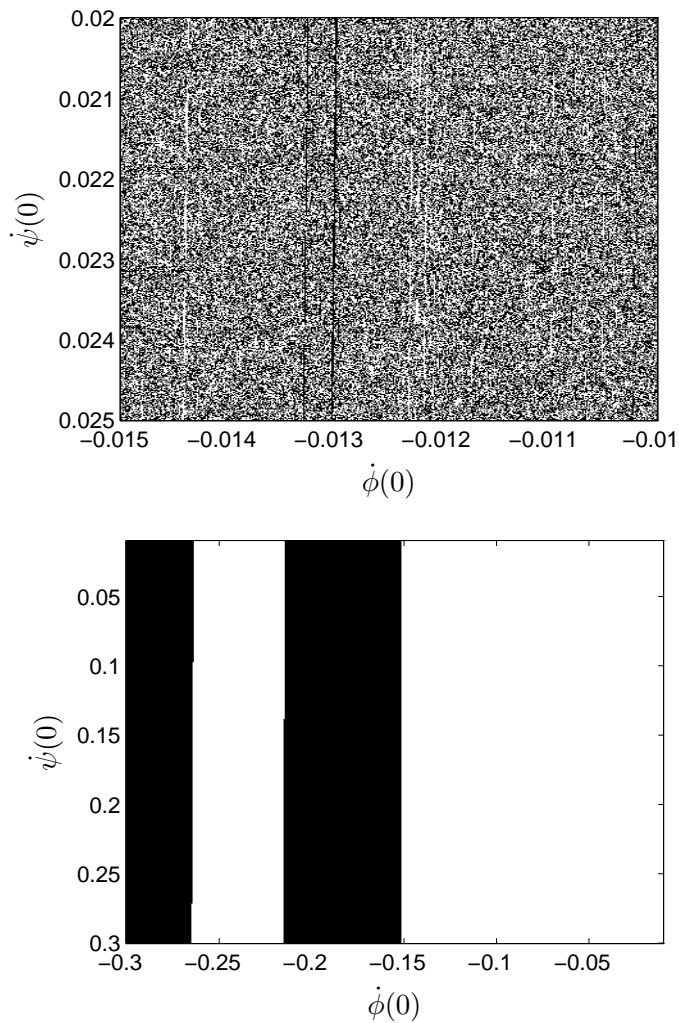


Figure 3: The minima of the potential reached at late times, as a function of initial conditions (for 420×420 equally spaced points), with $\phi(0) = \phi_{\text{inst}}$ and $\psi(0) = 0$. White points evolve towards the vacuum with $\psi > 0$. The upper plot shows the results for $\gamma = 0.5$, and those for $\gamma = 0$ are shown in the lower plot. Note the much larger range of initial data considered in the $\gamma = 0$ case. We have chosen $\dot{\phi}(0)$ negative so that ϕ is initially rolling “downhill”.

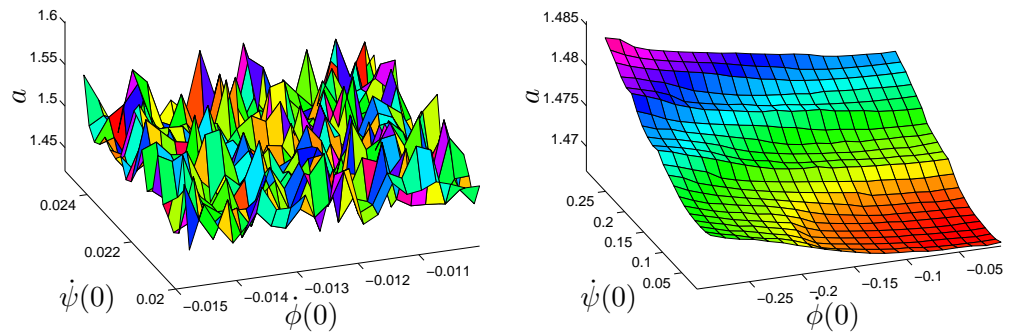


Figure 4: The scale factor at the moment the energy density becomes equal to M^4 and symmetry breaking occurs is plotted as a function of initial conditions, for $\gamma = 0.5$ (left) and $\gamma = 0$ (right). The scale factor, a , is normalized to be unity at the beginning of the integration. The initial data are the same as those used for fig. (3).

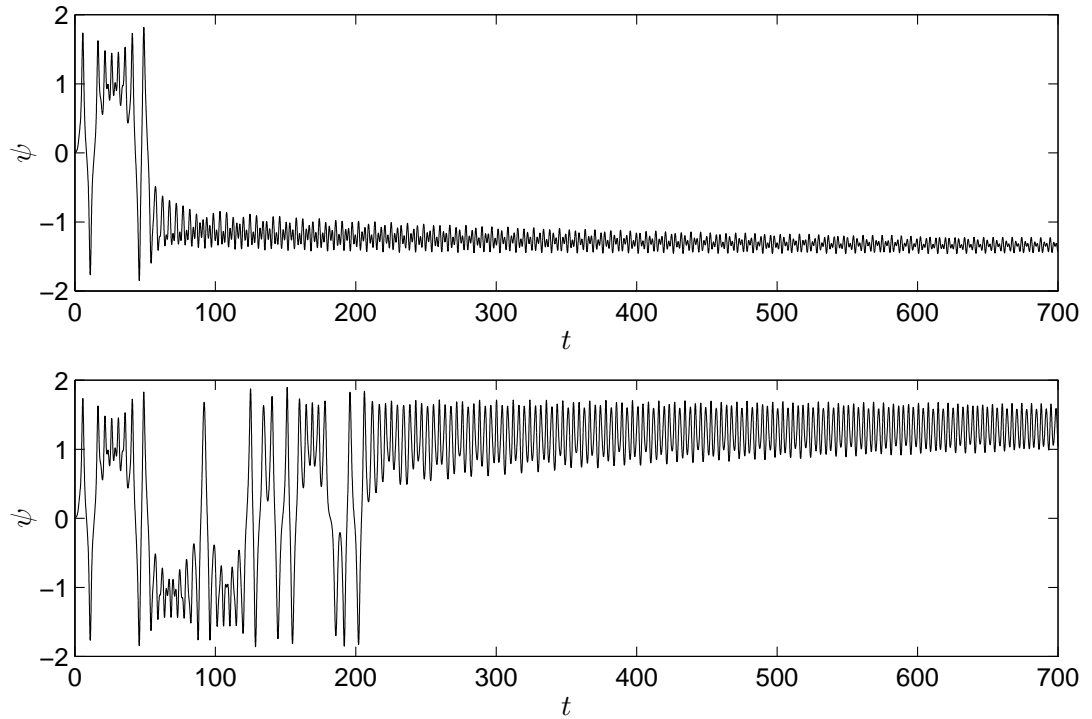


Figure 5: The evolution of ψ is plotted for two different initial conditions. In both cases the parameter values are the same as those used for the chaotic solutions in fig. (4), with the specific initial conditions $\dot{\psi} = .02$ and $\dot{\phi} = -0.01(1 + 1/419)$ (upper) and $\dot{\phi} = -0.01(1 + 2/419)$ (lower). The particular numerical values have been chosen to reproduce specific points in fig. (4).